



# Estimation of parametric convergence bounds for Volterra series expansion of nonlinear systems

Zhenlong Xiao, Xingjian Jing\*, Li Cheng

Department of Mechanical Engineering, Hong Kong Polytechnic University, Hung Hom, Kowloon, Hong Kong

## ARTICLE INFO

### Article history:

Received 21 May 2013

Received in revised form

14 November 2013

Accepted 21 November 2013

Available online 9 December 2013

### Keywords:

Parametric bound of convergence (PBoC)

Parametric convergence margin (PCM)

NARX model

Volterra series

Output frequency response

## ABSTRACT

The convergence bound for Volterra series expansion of nonlinear systems is investigated with a novel parametric approach in this study. To this aim, two fundamental concepts – parametric bound of convergence (PBoC) and parametric convergence margin (PCM) are proposed, which are related to the conditions, under which a given NARX model can be approximated by a convergent Volterra series, in terms of system characteristic parameters including model parameters (of interest), input magnitude, and frequency. The estimation of the PBoC and PCM is given in the frequency domain, which is expressed in terms of these characteristic parameters, and does not require iterative calculations. The results provide a fundamental basis for nonlinear analysis and design using Volterra series based methods, and also present a significant insight into understanding nonlinear influence (super/sub harmonics and modulation) with respect to model parameters and input magnitude. Several examples are given to illustrate the effectiveness of the results.

© 2013 Elsevier Ltd. All rights reserved.

## 1. Introduction

Many nonlinear systems can be identified into a Nonlinear AutoRegressive with eXogenous inputs (NARX) model [1–3], which includes several commonly-used nonlinear models as special cases. The NARX model actually provides a generic and convenient platform for analysis and design of nonlinear systems in practice. Given a parametric nonlinear model, several methods are available in the literature for nonlinear analysis and design [4–7]. For those systems described by NARX models, the nonlinear analysis and design can also be done in the frequency domain using the concept of Generalized Frequency Response Function (GFRF) [8]. The latter is defined as the multidimensional Fourier transform of Volterra kernels of the Volterra series expansion of the original nonlinear system. It is known that the input–output relationship of a considerably large class of nonlinear systems allows a Volterra series expansion [9–11,17,18]. For this reason, the Volterra series has been widely used in the literature for various nonlinear analysis and design [7,11–18].

Usually, the Volterra series expansion of the input–output relationship of a given NARX model should be confined into a specific region in order to ensure an accurate approximation of the original nonlinear dynamics. There are several results in the literature attempting to provide a convergence criterion under which a convergent Volterra series expansion exists. But some of these results are only applicable to specific nonlinear systems such as duffing oscillators [19–21], and others are either too general to apply for a specific parametric nonlinear model [9–12,17,18,22], or too conservative [23] or obviously over-estimated [19–21]. Noticeably, all existing results focus only on a convergent criterion in terms of input magnitude.

\* Corresponding author. Tel.: +852 2766 6680; fax: +852 2365 4703.

E-mail addresses: [xingjian.jing@polyu.edu.hk](mailto:xingjian.jing@polyu.edu.hk), [xingjian.jing@gmail.com](mailto:xingjian.jing@gmail.com) (X. Jing).

Nomenclature		$C(p, q)$	nonnegative function of model parameters
$\omega$	frequency variable	$c_{p,q}(k_1, \dots, k_{p+q})$	
$\Omega$	the output frequency	$M_p$	the maximum nonlinear degree in terms of output
$W_\infty$	the whole output frequency range	$L(\omega)$	lower bound of function $\ L_n(j\omega_1, \dots, j\omega_n)\ $
$U$	input magnitude	$\bar{Y}_{\Omega = k\omega}(U)$	upper bound of nonlinear output spectrum at $\Omega$ with input magnitude $U$
$c_{p,q}(k_1, \dots, k_{p+q})$	model parameters with nonlinear degree $p$ in terms of output and nonlinear degree $q$ in terms of input	$x = \bar{Y}(U)_\omega$	upper bound of the nonlinear output spectrum involves the whole output frequency range with input magnitude $U$ , which is denoted as $x$
$h_n(\tau_1, \dots, \tau_n)$	$n$ th order Volterra kernel	$C_n^m$	take $m$ combinations in the given $n$ elements
$L_n(j\omega_1, \dots, j\omega_n)$	the function of the linear model parameters $c_{1,0}(k_1)$	$\Gamma$	an indicator for convergence margin
$H_n(j\omega_1, \dots, j\omega_n)$	$n$ th order Generalized Frequency Response Function (GFRF)	PBoC	parametric bound of convergence
$\bar{H}_n(j\omega_1, \dots, j\omega_n)$	upper bound of $n$ th order GFRF	PCM	parametric convergence margin

In practical analysis and design of a nonlinear system, a fundamental problem could be: in what parameter ranges (in terms of the input magnitude or model parameters for a given input or at a given frequency) can the system have a convergent Volterra series expansion? More specifically, the task could only involve designing a particular model parameter. The question could be: under what range can the parameter take freely its value such that the system is always valid for a convergent Volterra series expansion? These practical questions are clearly key issues (for any nonlinear analysis and design using the Volterra series theory), but still not well addressed.

In this study, parametric convergent bounds in terms of some characteristic parameters including model parameters, magnitude bound of the first order GFRF (relating to linear model parameters), input magnitude, and frequency variables are studied for the NARX model in order to have a convergent Volterra series expansion. Firstly the analytical representation of the relationship between the upper bound of nonlinear output spectrum and characteristic parameters is presented. Then, the concept of parametric bound of convergence (PBoC) is discussed and the estimation of the PBoC for the NARX model is proposed, which clearly indicates in what parametric ranges a given nonlinear system has a convergent Volterra series expansion. Finally, a new convergence concept with respect to Volterra series expansion – parametric convergence margin (PCM) – is proposed, which can give a quantitative evaluation of the convergence margin in terms of any characteristic parameters for a given nonlinear system before the Volterra series expansion diverges. These new concepts and results should provide a significant basis and useful guidance for nonlinear analysis and design using the Volterra series based theory and methods [24–28], and can also present a new insight into understanding of nonlinear influence (e.g., super/sub-harmonic response) incurred by different characteristic parameters. Examples are given to illustrate these theoretical results.

## 2. Frequency response functions of nonlinear systems

### 2.1. The NARX model

Consider nonlinear systems described by the NARX model:

$$y(k) = \sum_{m=1}^M y_m(k) \tag{1a}$$

$$y_m(k) = \sum_{p=0}^m \sum_{(k_1, \dots, k_m)} c_{p,m-p}(k_1, \dots, k_m) \prod_{i=1}^p y(k-k_i) \prod_{i=p+1}^m u(k-k_i) \tag{1b}$$

where  $M$  is the maximum nonlinear degree in terms of  $y(k)$  and  $u(k)$ ,  $p$  is the nonlinear degree in terms of  $y(k)$ , and  $m-p$  is the nonlinear degree in terms of  $u(k)$  which is denoted later by  $q = m-p$ .  $(k_1, \dots, k_m)$  denotes all the combinations of nonlinear terms in terms of input and output, which can be expressed as  $(k_1, \dots, k_m) \in \mathfrak{S}_m = \{(k_1, \dots, k_m) | 1 \leq k_i \leq K, p \leq k_1 + \dots + k_p \leq pK, q \leq k_{p+1} + \dots + k_m \leq qK\}$ , where  $K$  is the maximum order of derivative, and  $c_{p,m-p}(k_1, \dots, k_m)$  is the corresponding coefficient of term  $\prod_{i=1}^p y(t-k_i) \prod_{i=p+1}^m u(t-k_i)$ . The NARX model (1) above can be approximated by a Volterra series expansion as [9–11,18]:

$$y(k) = \sum_{n=1}^N \int_{-\infty}^{\infty} \dots \int_{-\infty}^{\infty} h_n(\tau_1, \dots, \tau_n) \prod_{i=1}^n u(k-\tau_i) d\tau_i \tag{2}$$

where  $N$  is the truncation order, and  $h_n(\tau_1, \dots, \tau_n)$  is the  $n$ th order Volterra kernel.

## 2.2. The GFRF and nonlinear output spectrum

The  $n$ th order GFRF for the NARX model can be recursively calculated [24,28]:

$$H_n(j\omega_1, \dots, j\omega_n) = \frac{1}{L_n(\omega_1, \dots, \omega_n)} \sum_{m=1}^n \sum_{p=0, q=m-p}^m \sum_{(k_1, \dots, k_m)} c_{p,q}(k_1, \dots, k_m) e^{-\sum_{i=1}^q j\omega_{n-q+i} k_{p+i}} H_{n-q,p}(j\omega_1, \dots, j\omega_{n-q}) \quad (3)$$

$$L_n(\omega_1, \dots, \omega_n) = 1 - \sum_{k_1=1}^K c_{1,0}(k_1) e^{-jk_1 \sum_{i=1}^n \omega_i} \quad (4)$$

$$H_{n,p}(j\omega_1, \dots, j\omega_n) = \sum_{i=1}^{n-p+1} H_i(j\omega_1, \dots, j\omega_i) H_{n-i,p-1}(j\omega_{i+1}, \dots, j\omega_n) e^{-jk_p \sum_{j=1}^i \omega_j} \quad (5a)$$

or

$$H_{n,p}(j\omega_1, \dots, j\omega_n) = \sum_{r_1, \dots, r_p=1, \sum r_i=n}^{n-p+1} \prod_{i=1}^p H_{r_i}(j\omega_{X+1}, \dots, j\omega_{X+r_i}) e^{-jk_i \sum_{j=1}^{r_i} \omega_{X+j}} \quad (5b)$$

$$H_{n,1}(j\omega_1, \dots, j\omega_n) = H_n(j\omega_1, \dots, j\omega_n) e^{-jk_1 \sum_{i=1}^n \omega_i} \quad (6)$$

where  $H_{0,0}(\cdot) = 1$ ,  $H_{n,0}(\cdot) = 0$  for  $n > 0$ ,  $H_{n,p}(\cdot) = 0$  for  $n < p$ ,  $X = \sum_{j=1}^{i-1} r_j$  and

$$\exp\left(\sum_{i=1}^q j\omega_{n-q+i} k_{p+i}\right) = \begin{cases} 1 & q=0, p>1 \\ 0 & q=0, p \leq 1 \end{cases} \quad (7)$$

When  $n=1$ , the first order GFRF is the transfer function when all the nonlinear terms are zero, i.e.,

$$H_1(j\omega_1) = \frac{\sum_{k_1=1}^K c_{0,1}(k_1) e^{-j\omega_1 k_1}}{1 - \sum_{k_1=1}^K c_{1,0}(k_1) e^{-j\omega_1 k_1}} = \frac{\sum_{k_1=1}^K c_{0,1}(k_1) e^{-j\omega_1 k_1}}{L_1(j\omega_1)} \quad (8)$$

The nonlinear output spectrum subjected to a harmonic input

$$u(k) = U \cos(\omega T_s k + \angle A) = \frac{A}{2} e^{j\omega T_s k} + \frac{A^*}{2} e^{-j\omega T_s k} \quad (9)$$

where  $T_s$  is the sampling interval, can then be computed as follows [25]:

$$Y(j\Omega) = \sum_{n=1}^{+\infty} \frac{1}{2^n} \sum_{\omega_1 + \dots + \omega_n = \Omega} H_n(j\omega_1, \dots, j\omega_n) \prod_{i=1}^n A(\omega_i) \quad (10)$$

where  $\omega_i \in \{\omega, -\omega\}$ ,  $A(\omega) = A$ ,  $A(-\omega) = A^*$ , and  $U = |A|$ .

## 3. Bound of the output magnitude

### 3.1. Notations and definitions

The operator  $\|\cdot\|$  denotes the absolute value for scalars and Euclidian norm  $\|\cdot\|_2$  for vectors.  $\mathbb{N}$  is the set for all nonnegative integers, and  $\mathbb{N}^+$  for positive integers. Define

$$\underline{L}(\omega) = \inf_{\Omega \in W_\infty} \{\|L_n(j\omega_1, \dots, j\omega_n)\|\} \quad (11)$$

where  $W_\infty = \cup_{k=1}^{\infty} W_k = \cup_{k=1}^{\infty} \{\Omega | \Omega = \omega_1 + \dots + \omega_k, \omega_i \in \{\omega, -\omega\}\}$  [27].  $W_k$  is the set for all the output frequencies in the  $k$ th order output spectrum, and  $W_\infty$  represents the whole output frequency range when the NARX model subjects to excitation (9). Define

$$C(p, q) = \sum_{(k_1, \dots, k_m)} |c_{p,q}(k_1, \dots, k_m)| \quad (12)$$

where  $c_{p,q}(k_1, \dots, k_m)$  is the coefficient of the NARX model (1), and clearly  $C(p, q)$  is a nonnegative function. Denote

$$\bar{H}_1(j\omega_1) = \|H_1(j\omega_1)\| \quad (13)$$

### 3.2. Bound results for output spectrum

**Lemma 1.** For the upper bound of the  $n$ th order GFRF, it can be obtained as follows:

$$\sup\{\|H_n(j\omega_1, \dots, j\omega_n)\| | \forall \omega_1, \dots, \omega_n \in \{\omega, -\omega\}\} \leq \bar{H}_n(j\omega_1, \dots, j\omega_n)$$

$$= \frac{1}{\underline{L}(\omega)} \left( C(0, n) + \sum_{m=2}^n \sum_{p=1}^m C(p, q) \sum_{r_1, \dots, r_p=1}^{n-m+1} \prod_{\sum r_i = n-q}^p \bar{H}_{r_i}(\omega_{X+1}, \dots, \omega_{X+r_i}) \right), \quad n \geq 2 \quad (14)$$

**Proof.** See Lemma 1 in [26]. □

**Lemma 2.** The upper bound of the nonlinear output spectrum for the whole output frequency range  $W_\infty$  is given as follows:

$$\bar{Y}(U)_\omega = \sum_{k=0}^{\infty} \bar{Y}_{\Omega=k\omega}(U) = \sum_{\Omega \in W_\infty} \bar{Y}_\Omega(U) = \sum_{n=1}^{\infty} \|\sum_{\Omega \in W_n} \bar{Y}_n(j\Omega)\| = \sum_{n=1}^{+\infty} \bar{H}_n(j\omega_1, \dots, j\omega_n) U^n \quad (15)$$

where  $\bar{Y}_{\Omega=k\omega}(U)$  is the upper bound of the output spectrum at frequency  $\Omega = k\omega, k \in \mathbb{N}$ , which is given as follows:

$$|Y(j\Omega)| \leq \bar{Y}_{\Omega=k\omega}(U) = \sum_{n=1}^{\infty} \frac{C_{k+2(n-1)}^{n-1}}{2^{k+2(n-1)-1}} \bar{H}_{k+2(n-1)}(j\omega_1, \dots, j\omega_{k+2(n-1)}) U^{k+2(n-1)} \quad k \in \mathbb{N}^+ \quad (16a)$$

$$|Y(j\Omega)| \leq \bar{Y}_{\Omega=k\omega}(U) = \sum_{n=1}^{\infty} \frac{C_{2n}^n}{2^{2n}} \bar{H}_{2n}(j\omega_1, \dots, j\omega_{2n}) U^{2n} \quad k = 0 \quad (16b)$$

**Proof.** Following discussions in [29]. □

**Proposition 1.** The analytical relationship among the upper bound of nonlinear output spectrum, model parameters, magnitude bound of the first order GFRF, input magnitude, and frequency variable, can be obtained as follows:

$$\sum_{p=1}^{M_p} \left( \sum_{q=0}^{\infty} C(p, q) U^q \right) x^p - \underline{L}(\omega)x + \left( \underline{L}(\omega)\bar{H}_1(j\omega)U + \sum_{m=2}^{\infty} C(0, m)U^m \right) = 0, \quad p+q \geq 2 \quad (17)$$

where  $x$  is denoted for  $x(\omega, U)$  and  $x(\omega, U) = \bar{Y}(U)_\omega = \sum_{n=1}^{+\infty} \bar{H}_n(j\omega_1, \dots, j\omega_n) U^n$ ,  $M_p$  is the maximum nonlinear degree in terms of output variable  $y(k)$ . Specifically, when the NARX model involves only those nonlinear terms with  $p = 1$  or together with the pure input nonlinearity, the upper bound of nonlinear output spectrum  $x$  can be obtained directly as follows:

$$x = \frac{\bar{H}_1(j\omega)U + (1/\underline{L}(\omega))\sum_{q=m=2}^{\infty} C(0, m)U^m}{1 - (1/\underline{L}(\omega))\sum_{q=1}^{\infty} C(1, q)U^q}. \quad (18)$$

**Proof.** See Appendix A. □

**Remark 1.** The output bound  $x$  in (17) should be a real nonnegative number. If (17) possesses only one positive root, it is clearly the output bound of the NARX model (1); when (17) has more than two positive roots, the parametric convergence margin proposed later can help to determine the true output bound.

#### 4. Parametric bound of convergence (PBoC)

The parametric bound of convergence (PBoC) is referred to here as a bound (e.g.,  $\bar{C}$ ) for any characteristic parameter  $C$  (i.e.,  $\|C\| \leq \bar{C}$ ) under which the NARX model has a convergent Volterra series expansion.

**Proposition 2.** A formal function  $\Gamma(x; C, U, \omega)$  (which is a function of the upper bound of the nonlinear output spectrum  $x$ , the frequency variable  $\omega$ , and the input amplitude  $U$ , and denoted as  $\Gamma$  in what follows), is given as follows:

$$\Gamma = \frac{1}{\underline{L}(\omega)} \sum_{p=1}^{M_p} \sum_{q=0}^{\infty} pC(p, q)U^q x^{p-1}, \quad p+q \geq 2 \quad (19)$$

Then, the upper bound of the nonlinear output spectrum, i.e., the power series  $x = \sum_{n=1}^{+\infty} \bar{H}_n(j\omega_1, \dots, j\omega_n) U^n$  is convergent when  $0 \leq \Gamma < 1$ , and divergent when  $\Gamma \geq 1$ .

**Proof.** See Appendix B. □

**Remark 2.** The function  $\Gamma$  is a nonnegative continuous and monotonically increasing function of  $C(p, q)$  or the input amplitude  $U$ .

**Remark 3.** When the NARX model (1) has only pure input nonlinearity, then the whole input part can be considered as a new input. In this case, the model can be regarded as a linear model with this new input, which is not focused in this study.

**Proposition 3.** Consider the NARX model except the case that the NARX model involves only the nonlinear terms with index  $p=1$ , or together with only pure input nonlinear terms, the analytical PBoC can be obtained by solving the following equation:

$$\begin{aligned}
 & \left. \begin{array}{l} M_p - 1 \text{ rows} \\ \\ \\ \end{array} \right\} \begin{array}{l} \left| \begin{array}{ccccccc} a_{1,M_p} & a_{1,M_p-1} & \cdots & a_{1,0} & 0 & \cdots & 0 \\ 0 & a_{1,M_p} & a_{1,M_p-1} & \cdots & a_{1,0} & \cdots & 0 \\ & & \cdots & & & & \\ 0 & 0 & \cdots & a_{1,M_p} & a_{1,M_p-1} & \cdots & a_{1,0} \end{array} \right| \\ \end{array} = 0 \\
 & \left. \begin{array}{l} M_p \text{ rows} \\ \\ \\ \end{array} \right\} \begin{array}{l} \left| \begin{array}{ccccccc} a_{2,M_p-1} & a_{2,M_p-2} & \cdots & a_{2,0} & 0 & \cdots & 0 \\ 0 & a_{2,M_p-1} & a_{2,M_p-2} & \cdots & a_{2,0} & \cdots & 0 \\ & & \cdots & & & & \\ 0 & 0 & \cdots & a_{2,M_p-1} & a_{2,M_p-2} & \cdots & a_{2,0} \end{array} \right| \\ \end{array} = 0
 \end{aligned} \tag{20}$$

where  $M_p$  takes the same definition as in Proposition 1, and

$$a_{1,p} = \left( (p-1) \sum_{q=0}^{\infty} C(p,q)U^q \right), \quad 1 \leq p \leq M_p, p+q \geq 2, \tag{21a}$$

$$a_{1,0} = - \left( \underline{L}(\omega) \bar{H}_1(j\omega)U + \sum_{m=2}^{\infty} C(0,m)U^m \right), \tag{21b}$$

$$a_{2,p-1} = p \sum_{q=0}^{\infty} C(p,q)U^q, \quad 2 \leq p \leq M_p, \tag{21c}$$

$$a_{2,0} = \sum_{q=1}^{\infty} C(1,q)U^q - \underline{L}(\omega). \tag{21d}$$

Particularly, when the NARX model (1) involves only nonlinear terms with index  $p=1$  or together with the pure input nonlinear terms, the PBoC can be obtained by directly solving  $\Gamma=1$ , that is,

$$\frac{1}{\underline{L}(\omega)} \sum_{q=1}^{\infty} C(1,q)U^q = 1. \tag{22}$$

**Proof.** See Appendix C.  $\square$

**Remark 4.** It is interesting to see that if the NARX model involves only nonlinear terms with index  $p=1$  or  $p=0$ , the coefficients of the pure input nonlinearity do not take a role in (19), which means that these nonlinearities do not affect the convergence bound. But except this case, the pure input nonlinearities could have great influence on the convergence bound, which can be seen from (20) and (21b), and will also be validated in Sections 6.3 and 6.4.

**Remark 5.** When the input amplitude  $U$  is given, from (20) the PBoC of any model parameter of interest can be obtained. When the parameter values are selected under the bound calculated by (20), the nonlinear system can be well approximated by a convergent Volterra series. When all the model parameters are given, the PBoC of the input amplitude can be obtained. The latter has been studied in [19–23,29] for some specific nonlinear systems. The result in Proposition 3 is more general, not restrictive to any specific nonlinearity, and also less conservative due to the frequency dependent bound used. This will be further discussed in Section 6.

**Algorithm 1.** Computation of PBoC:

- Step 1.** Calculate  $\underline{L}(\omega)$  according to (4) and (11); calculate  $\bar{H}_1(j\omega_1)$  according to (8) and (13); calculate  $C(p,q)$  using (12).
- Step 2.** Compute (21) to construct (20) for the applicable case.
- Step 3.** Solve (20) or (22) for the applicable case to obtain the PBoC.

## 5. The parametric convergence margin (PCM)

Practical systems always undergo various perturbations. If the values of model parameters are chosen very close to the PBoC, the dynamic response of the nonlinear system under study would be easier to go astray from a Volterra series expansion. Therefore, for any characteristic parameter, it is reasonable to develop a measure for assessing the convergence margin in terms of this parameter, which is referred to here as the parametric convergence margin (PCM), before the Volterra series expansion diverges. A larger PCM implies that the system dynamics can be well approximated by a Volterra series expansion and stays away from its divergence.

Considering the function  $\Gamma$  in (19), when all the nonlinear coefficients in the NARX model are equal to 0 or the input amplitude  $U=0$ , then  $\Gamma=0$ ; when the nonlinear coefficients or the input amplitude reach the PBoC, then  $\Gamma=1$ ; when the

nonlinear coefficients or the input amplitude is out of the PBoC, then  $\Gamma > 1$ . Because of these properties, the function  $\Gamma$  can be used as an overall indicator to the convergence margin of the NARX model. Therefore, the PCM is defined as follows:

$$\text{PCM} = 1 - \Gamma \tag{23}$$

When the PCM is very close to 1, the NARX model possesses the largest convergence margin; when the PCM is close to 0, the NARX model is very close to the convergent bound and has smaller convergence margin; when the PCM is negative, the system cannot be expanded by a Volterra series and thus is not a Volterra-type system.

The function  $\Gamma$  in (19) involves the iterative computation (the computation of the upper bound of nonlinear output spectrum  $x$ ). In order to eliminate the iteration, the following result is needed.

**Proposition 4.** *When the NARX model does not only possess nonlinear terms with index  $p=1$  or together with pure input nonlinearity, the indicator  $\Gamma$  can be obtained by solving*

$$\begin{aligned} M_p - 1 \text{ rows} & \left\{ \begin{array}{ccccccc} a_{1,M_p} & a_{1,M_p-1} & \cdots & a_{1,0} & 0 & \cdots & 0 \\ 0 & a_{1,M_p} & a_{1,M_p-1} & \cdots & a_{1,0} & \cdots & 0 \\ & & \cdots & & & & \\ 0 & 0 & \cdots & a_{1,M_p} & a_{1,M_p-1} & \cdots & a_{1,0} \end{array} \right\} = 0 \\ M_p \text{ rows} & \left\{ \begin{array}{ccccccc} a_{2,M_p-1} & a_{2,M_p-2} & \cdots & a_{2,0} & 0 & \cdots & 0 \\ 0 & a_{2,M_p-1} & a_{2,M_p-2} & \cdots & a_{2,0} & \cdots & 0 \\ & & \cdots & & & & \\ 0 & 0 & \cdots & a_{2,M_p-1} & a_{2,M_p-2} & \cdots & a_{2,0} \end{array} \right\} = 0 \end{aligned} \tag{24}$$

where  $M_p$  is the same as before, and

$$a_{1,p} = \sum_{q=0}^{\infty} C(p, q)U^q, \tag{25a}$$

$$a_{1,1} = \sum_{q=1}^{\infty} C(1, q)U^q - \underline{L}(\omega), \tag{25b}$$

$$a_{1,0} = \underline{L}(\omega)\bar{H}_1(j\omega)U + \sum_{m=2}^{\infty} C(0, m)U^m, \tag{25c}$$

$$a_{2,p-1} = p \sum_{q=0}^{\infty} C(p, q)U^q, \tag{25d}$$

$$a_{2,0} = \sum_{q=1}^{\infty} C(1, q)U^q - \Gamma \underline{L}(\omega). \tag{25e}$$

where  $2 \leq p \leq M_p$ . Specifically, when the NARX model possesses only nonlinear terms with index  $p=1$  or together with pure input nonlinearity,  $\Gamma$  can be directly obtained according to (19) because in this case  $\Gamma$  does not involve the iterative computation of  $x$ .

**Proof.** See Appendix D.  $\square$

**Remark 6.** When  $0 \leq \Gamma < 1$ , it implies that the NARX model which possesses unique steady state can be well approximated by a convergent Volterra series, i.e.,  $0 < \text{PCM} \leq 1$ ; when  $\Gamma \geq 1$ , i.e.,  $\text{PCM} \leq 0$ , the Volterra series becomes divergent and then cannot approximate to the NARX model. From (19), it is clear that  $\Gamma$  is a real nonnegative number. Therefore, if (24) has no real positive root, the nonlinear model of interest can be seen as divergent in the sense of Volterra series expansion. If there exists more than one real positive root, the PBoC can be used to determine the true  $\Gamma$  for the nonlinear system. That is, when the nonlinear coefficients are out of the PBoC, the solution larger than 1 should be the true  $\Gamma$ ; otherwise, the solution smaller than 1 is the true one. Similarly, when there exist more than one real positive solutions for (17), the solutions can be substituted into (19) for calculating  $\Gamma$ , the true solution for output bound  $x$  should be the one who has the same  $\Gamma$  by (19) as that obtained by (24).

**Remark 7.** It must be pointed out that, although the results developed in this study consider only a harmonic input, similar results could be extended to more complicated cases considering general input signals by following similar techniques, which will be done in a further investigation. Moreover, from the numerical examples below it can be seen that the PBoC and PCM provide a very novel point of view for understanding of nonlinear influence on system dynamic response (such as super/sub harmonics and modulation) incurred by different characteristic parameters. Some other recent advances also vindicate that the Volterra series approach can also be used for interpretation of complicated nonlinear behavior such as bifurcation and even chaos [21,30,31].

**Remark 8.** There are some other nonlinear analysis methods, such as, harmonic balance methods and nonlinear normal mode [4], which are often computationally intensive as the nonlinear degree of the system increases [5,6]. This study

presents a simple and novel evaluation on the nonlinear influence in terms of characteristic parameters and on the parametric convergence bound of a nonlinear system in the sense of Volterra series expansion. This provides a very fundamental but significant basis for nonlinear analysis and design using the Volterra series based methods [7,24–28,32].

To facilitate the computation of the PCM, the following procedure can be used.

**Algorithm 2.** Computation of PCM:

- Step 1.** Calculate  $\underline{L}(\omega)$  according to (4) and (11); Calculate  $\overline{H}_1(j\omega_1)$  according to (8) and (13); Calculate  $C(p, q)$  from (12).
- Step 2.** Compute (25) to construct (24) for the applicable case.
- Step 3.** Solve (24) or (19) for the applicable case to obtain the indicator  $\Gamma$ .
- Step 4.** Calculate (23) for the applicable case to obtain the PCM.

## 6. Examples and discussions

In order to illustrate the theoretical results, the NARX model in four cases with different nonlinear terms are discussed, which is given with zero initial conditions as follows:

$$y(k) = c_{1,0}(1)y(k-1) + c_{1,0}(2)y(k-2) + c_{3,0}(1, 1, 1)y^3(k-1) + c_{1,2}(1, 1, 1)y(k-1)u^2(k-1) + c_{0,3}(1, 1, 1)u^3(k-1) + c_{0,1}(1)u(k-1). \quad (26)$$

The model in (28) can be obtained by discretizing in a backward manner the following nonlinear differential equation:

$$m\ddot{y}(t) + c\dot{y}(t) + k_1y(t) + k_{30}y^3(t) + k_{12}y(t)u^2(t) + k_{03}u^3(t) = u(t) \quad (27)$$

where the linear part coefficients are given as  $m = 1, c = 0.01\omega_0, k_1 = \omega_0^2, \omega_0 = 20\pi$ , and  $u(t) = U \cos(\omega t)$ . Setting  $T_s = 1/2000$  s, then  $u(k) = U \cos(\Omega k) = U \cos(\omega T_s k)$  and  $c_{1,0}(1) = 2 - (cT_s/m) - (kT_s^2/m) = 1.9987, c_{1,0}(2) = (cT_s/m) - 1 = -0.9997, c_{0,1}(1) = (T_s^2/m) = 2.5 \times 10^{-7}, c_{3,0}(1, 1, 1) = -(k_{30}T_s^2/m), c_{1,2}(1, 1, 1) = -(k_{12}T_s^2/m), c_{0,3}(1, 1, 1) = -(k_{03}T_s^2/m)$ .

The discussion starts with the case that the NARX model only possesses pure output nonlinear terms, that is,  $c_{1,2}(1, 1, 1) = c_{0,3}(1, 1, 1) = 0$ , which can be obtained by discretizing the well-known Duffing oscillator equation. Several existing results available in the literature are compared for this example. However, no existing results can be applied to the following examples. In Section 6.2, the nonlinear term with coefficient  $c_{1,2}(1, 1, 1)$  is additionally considered in the discussion. That is, only  $c_{0,3}(1, 1, 1)$  is set to be zero in (26). Section 6.3, is to illustrate and validate Remark 4 (the pure nonlinear term in the case pointed by Remark 4 does not affect the PBoC and PCM), and thus considers that the NARX model has only nonlinear terms with index  $p=1$  and a pure input nonlinear term. Finally, the NARX model with pure output nonlinearity and pure input nonlinearity, that is, only  $c_{1,2}(1, 1, 1) = 0$  in model (26), is discussed in Section 6.4, which is used to verify Remark 4 again, that is, except the case pointed by Remark 4, the pure input nonlinear term could greatly affect the PBoC and PCM.

It can be shown that when all the parameters of the NARX model are given, (20) or (22) can also give an estimation of the PBoC for the input amplitude. But this paper focuses on the PBoC for model parameters and the PCM.

In order to indicate the error between the synthesized output using Volterra series and the real output, the Normalized Root Mean Square Error (NRMSE) is introduced,

$$\text{NRMSE} = \sqrt{\frac{\sum (y_{\text{synthesized}}(k) - y_{\text{real}}(k))^2}{\sum (y_{\text{real}}(k))^2}} \quad (28)$$

where  $y_{\text{synthesized}}$  is the synthesized output and  $y_{\text{real}}(k)$  is the real output.

### 6.1. The NARX model with pure output nonlinearity

The model is given by the following:

$$y(k) = c_{1,0}(1)y(k-1) + c_{1,0}(2)y(k-2) + c_{3,0}(1, 1, 1)y^3(k-1) + c_{0,1}(1)u(k-1) \quad (29)$$

which can be obtained by discretizing the well-known Duffing equation. The PBoC of  $c_{3,0}(1, 1, 1)$  is calculated firstly, and then when the coefficient  $c_{3,0}(1, 1, 1)$  and the input are given, the PCM of the NARX model is discussed. The linear coefficients and input are given as before after Eq. (26).

The PBoC of  $c_{3,0}(1, 1, 1)$  can be computed with Algorithm 1. According to (21), it gives,

$$\begin{aligned} a_{1,3} &= 2C(3, 0), a_{1,0} = -\overline{H}_1(j\omega)UL(\omega), \\ a_{2,2} &= 3C(3, 0), a_{2,0} = -\underline{L}(\omega), \\ a_{1,2} &= a_{1,1} = a_{2,1} = 0. \end{aligned}$$

where  $C(3,0) = |c_{3,0}(1, 1, 1)|$ . Then from (20), the bound satisfies the following equation:

$$\begin{vmatrix} 2C(3,0) & 0 & 0 & -\bar{H}_1(j\omega)U\underline{L}(\omega) & 0 \\ 0 & 2C(3,0) & 0 & 0 & -\bar{H}_1(j\omega)U\underline{L}(\omega) \\ 3C(3,0) & 0 & -\underline{L}(\omega) & 0 & 0 \\ 0 & 3C(3,0) & 0 & -\underline{L}(\omega) & 0 \\ 0 & 0 & 3C(3,0) & 0 & -\underline{L}(\omega) \end{vmatrix} = 0. \tag{30}$$

By denoting

$$A = \begin{pmatrix} 2C(3,0) & 0 \\ 0 & 2C(3,0) \end{pmatrix}, \quad B = \begin{pmatrix} 0 & -\bar{H}_1(j\omega)U\underline{L}(\omega) & 0 \\ 0 & 0 & -\bar{H}_1(j\omega)U\underline{L}(\omega) \end{pmatrix},$$

$$C = \begin{pmatrix} 3C(3,0) & 0 \\ 0 & 3C(3,0) \\ 0 & 0 \end{pmatrix}, \quad D = \begin{pmatrix} -\underline{L}(\omega) & 0 & 0 \\ 0 & -\underline{L}(\omega) & 0 \\ 3C(3,0) & 0 & -\underline{L}(\omega) \end{pmatrix}, \tag{30}$$

is equivalent to  $|A||D - CA^{-1}B| = 0$ . Because  $C(3,0)$  is positive, from (30) the following equation holds:

$$\underline{L}(\omega) - \frac{27}{4}C(3,0)(\bar{H}_1(j\omega)U)^2 = 0. \tag{31}$$

From Eq. (31),  $C(3,0)$  can be solved, which is the PBoC of  $c_{3,0}(1, 1, 1)$  in terms of the input amplitude  $U$ , and the linear part magnitude (i.e.,  $\underline{L}(\omega)$  and  $\bar{H}_1(j\omega)$ ). If the input and all the linear coefficients are given, then clearly the PBoC can be obtained. Similarly, if all the coefficients of the model are given, the PBoC for the input can also be computed by (31).

In the simulation, the input amplitude is given as  $U = 0.5$ .  $\underline{L}(\omega)$  and  $\bar{H}_1(j\omega)$  can be obtained from (11) and (13), respectively. From (11), it can be obtained that  $\underline{L}(\omega) = \inf \{L(\omega), L(3\omega), L(5\omega), L(7\omega), \dots\}$  [32]. Since the first several orders of output spectra take the dominant roles, it can be simplified as  $\underline{L}(\omega) = \inf \{L(\omega), L(3\omega), L(5\omega), L(7\omega)\}$  [27,32]. The estimated PBoC of  $|c_{3,0}(1, 1, 1)|$  is shown in Fig. 1, indicating a very close estimation to the real ones (obtained by numerical simulations) at different frequencies. The estimated bound varies a lot at different frequency and tends to be small at or around harmonic resonance frequencies. This shows clearly the nonlinear influence and potential behavior (Volterra or bifurcation, etc.) due to this specific nonlinearity.

To validate the effectiveness of the convergent bound above, a comparison between the model with the estimated bound and the model with a larger nonlinear coefficient  $|c_{3,0}(1, 1, 1)|$  is given in Fig. 2. The comparison is chosen for example at  $\omega = 0.8\omega_0$  (to show the accuracy of the estimation around the resonant frequency in what follows). At this frequency, the estimated PBoC is  $C(3,0) = 426.0788$ . Fig. 2 shows that when the coefficient  $c_{3,0}(1, 1, 1) = -426.0788$ , the synthesized output and the real output has a good agreement (with the NRMSE quickly decreasing to 0 as the synthesized order increases), while for a larger nonlinear coefficient  $|c_{3,0}(1, 1, 1)|$ , the synthesized output becomes slowly divergent with increased NRMSE.

For comparison with other existing results [19–21,23], the PBoCs for the input amplitude obtained with different methods are given in Fig. 3, which indicate that our result provides the closest estimation. It should be noted that all the existing results can only be used to find an estimation of the PBoC for the input amplitude, while for the nonlinear systems in cases B-D that will be shown later, the existing results are not applicable.

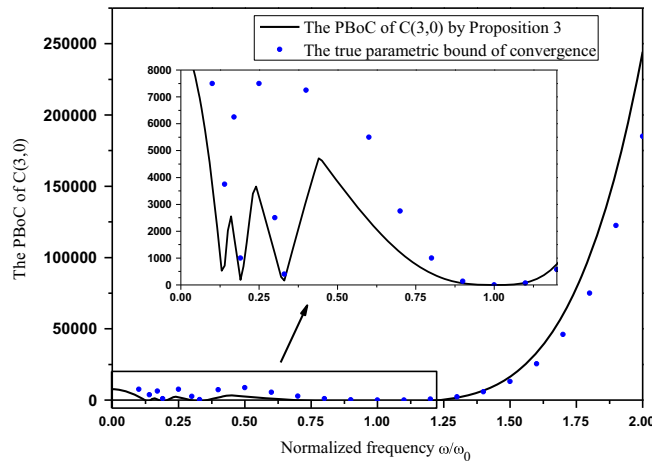


Fig. 1. The PBoC of  $C(3,0) = |c_{3,0}(1, 1, 1)|$ .



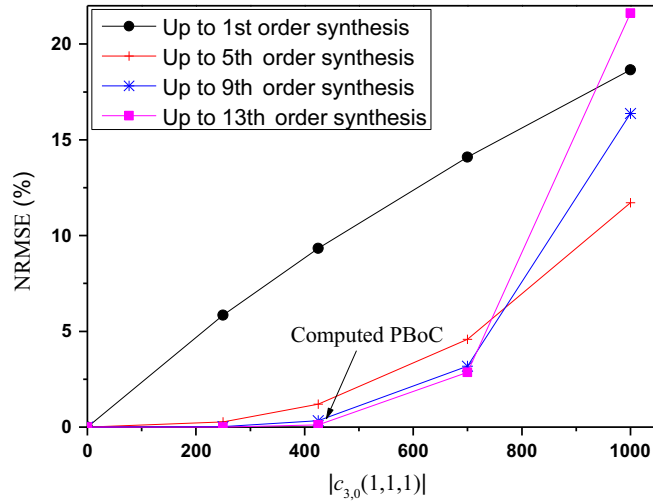


Fig. 2. Comparison of the synthesized output and the original output at  $\omega = 0.8\omega_0$ .

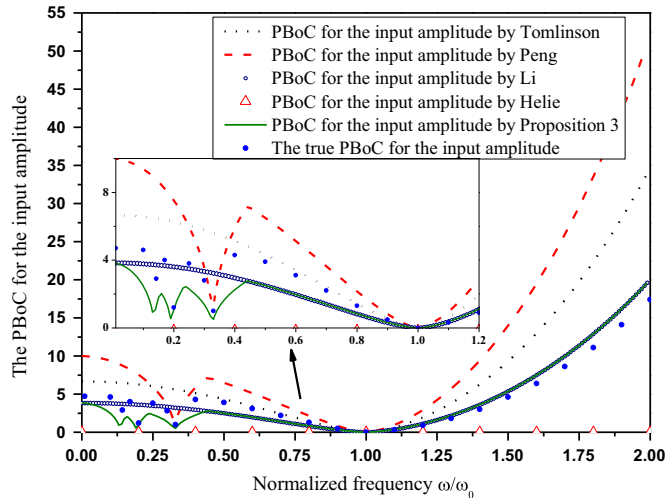


Fig. 3. The PBoCs for the input amplitude.

The following discussion is to show the convergence margin, PCM, which can follow Algorithm 2. From the analysis above, (24) is applicable for this case. According to (25), the following equations hold:

$$\begin{aligned} a_{1,3} &= C(3, 0), & a_{1,1} &= -\underline{L}(\omega), & a_{1,0} &= \overline{H}_1(j\omega)U\underline{L}(\omega) \\ a_{2,2} &= 3C(3, 0), & a_{2,0} &= -\Gamma\underline{L}(\omega) \\ a_{1,2} &= a_{2,1} = 0. \end{aligned}$$

Then  $\Gamma$  can be estimated from (24), that is,

$$\begin{vmatrix} C(3,0) & 0 & -\underline{L}(\omega) & \overline{H}_1(j\omega)U\underline{L}(\omega) & 0 \\ 0 & C(3,0) & 0 & -\underline{L}(\omega) & \overline{H}_1(j\omega)U\underline{L}(\omega) \\ 3C(3,0) & 0 & -\Gamma\underline{L}(\omega) & 0 & 0 \\ 0 & 3C(3,0) & 0 & -\Gamma\underline{L}(\omega) & 0 \\ 0 & 0 & 3C(3,0) & 0 & -\Gamma\underline{L}(\omega) \end{vmatrix} = 0. \quad (32)$$

From (32), the following equation can be obtained:

$$\Gamma^3 - 6\Gamma^2 + 9\Gamma - \frac{27C(3,0)(\overline{H}_1(j\omega)U)^2}{\underline{L}(\omega)} = 0. \quad (33)$$

From (33),  $\Gamma$  can be solved, which should be a real number. Then the PCM can be obtained according to (23). The convergence margin when for example  $c_{3,0}(1, 1, 1) = -153.8223$  and  $U = 0.5$  is presented in Fig. 4.

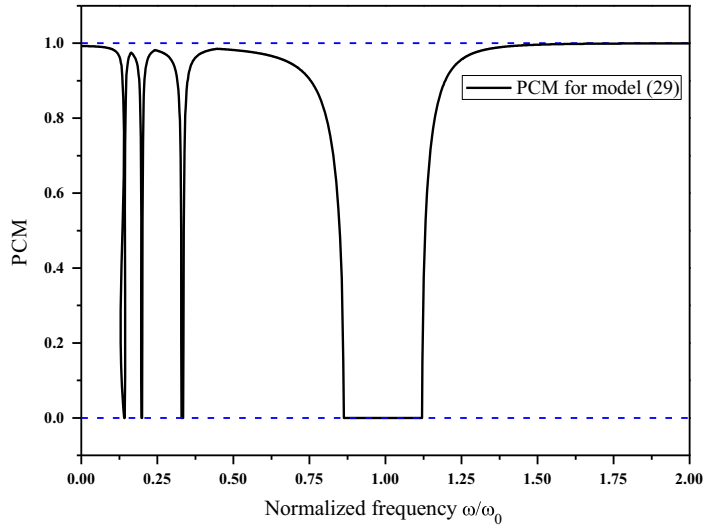


Fig. 4. The parametric convergence margin (PCM) for model (29).

Around the resonant frequency, the PCM is equal to zero, which means that the nonlinear system with given coefficients and input is divergent in the sense of Volterra series expansion, while at high frequencies the PCM is near to 1. This is consistent with the previous PBoC results, and also confirms the existing knowledge about the Duffing equation [19,21] regarding harmonic response. Numerical simulations can verify that complicated nonlinear behaviors (e.g., bifurcation) can be observed in the frequency band where PCM = 0.

6.2. The NARX model with pure output nonlinearity and cross nonlinearity

In this example, the NARX model has a nonlinear cross-term with  $p=1$  and also has a pure output nonlinear term with  $p=3$ , i.e.,

$$y(k) = c_{1,0}(1)y(k-1) + c_{1,0}(2)y(k-2) + c_{3,0}(1, 1, 1)y^3(k-1) + c_{1,2}(1, 1, 1)y(k-1)u^2(k-1) + c_{0,1}(1)u(k-1) \tag{34}$$

Following Algorithm 1 gives the PBoC. From (21), it can be obtained that,

$$\begin{aligned} a_{1,3} &= 2C(3, 0), & a_{1,0} &= -\bar{H}_1(j\omega)U\underline{L}(\omega), \\ a_{2,2} &= 3C(3, 0), & a_{2,0} &= C(1, 2)U^2 - \underline{L}(\omega), \\ a_{1,2} &= a_{1,1} = a_{2,1} = 0. \end{aligned}$$

where  $C(3, 0) = |c_{3,0}(1, 1, 1)|$ , and  $C(1, 2) = |c_{1,2}(1, 1, 1)|$ . Then according to (20), it gives,

$$\begin{vmatrix} 2C(3, 0) & 0 & 0 & -\bar{H}_1(j\omega)U\underline{L}(\omega) & 0 \\ 0 & 2C(3, 0) & 0 & 0 & -\bar{H}_1(j\omega)U\underline{L}(\omega) \\ 3C(3, 0) & 0 & C(1, 2)U^2 - \underline{L}(\omega) & 0 & 0 \\ 0 & 3C(3, 0) & 0 & C(1, 2)U^2 - \underline{L}(\omega) & 0 \\ 0 & 0 & 3C(3, 0) & 0 & C(1, 2)U^2 - \underline{L}(\omega) \end{vmatrix} = 0 \tag{35}$$

Similarly to Section 6.1, by partitioning the matrix and computing the determinant in (35), it can be obtained (considering  $C(3, 0)$  and  $C(1, 2)$  are positive) that,

$$(C(1, 2)U^2 - \underline{L}(\omega))^3 + \frac{27}{4}C(3, 0)(\bar{H}_1(j\omega)U\underline{L}(\omega))^2 = 0 \tag{36}$$

Clearly, (36) provides an analytical relationship among the parametric bounds involving several parameter magnitudes, i.e.,  $C(3, 0), C(1, 2), U$ , and the linear part of the model. Given all the other parameter magnitudes, the PBoC of the remaining one can thus be obtained. Therefore, it can be obtained that

$$C(1, 2) = \frac{\underline{L}(\omega) - \sqrt[3]{(27/4)C(3, 0)(\bar{H}_1(j\omega)U\underline{L}(\omega))^2}}{U^2}. \tag{37}$$

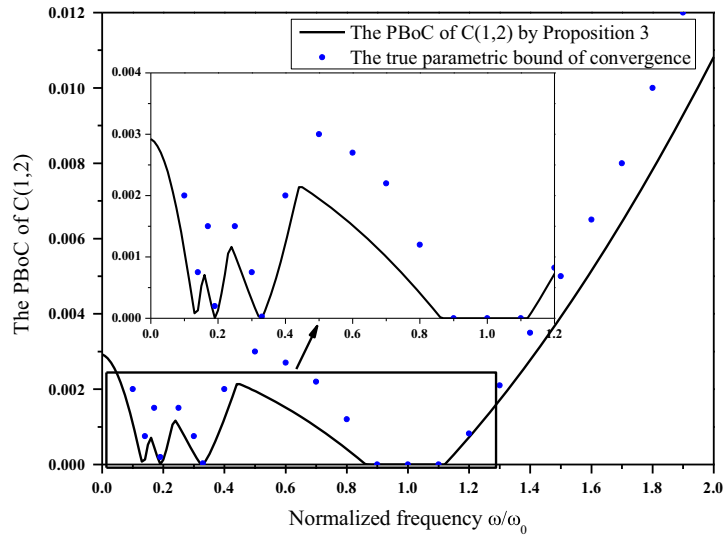


Fig. 5. The PBoC of  $C(1,2) = |c_{1,2}(1, 1, 1)|$ .

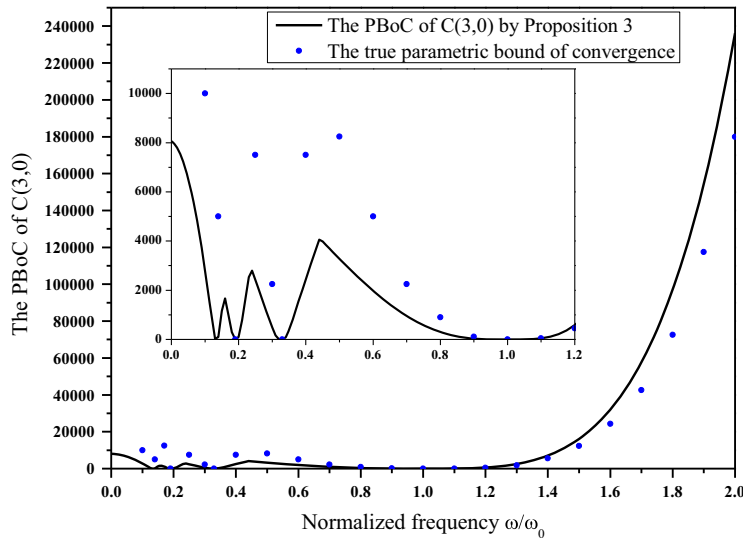


Fig. 6. The PBoC of  $C(3,0) = |c_{3,0}(1, 1, 1)|$ .

$$C(3,0) = \frac{4 (\underline{L}(\omega) - C(1,2)U^2)^3}{27 (\overline{H}_1(j\omega)U\underline{L}(\omega))^2}. \tag{38}$$

In the simulation, the input amplitude is set to  $U = 0.5$ ,  $c_{3,0}(1, 1, 1) = -153.8223$  for (37), and  $c_{1,2}(1, 1, 1) = -1.5382 \times 10^{-4}$  for (38). The estimated bound results are presented in Figs. 5 and 6. In Fig. 5, it is shown that at or around the resonant frequency or some harmonic resonance frequencies, the PBoC for  $C(1,2)$  is zero, which means that the model with  $c_{3,0}(1, 1, 1) = -153.8223$ ,  $c_{1,2}(1, 1, 1) = 0$ , and  $U = 0.5$  has no convergent Volterra series expansion; Similar phenomena can also be observed in Fig. 6 for the PBoC of  $C(3,0)$ .

Similar to Section 6.1, to validate the effectiveness of the estimated bounds, take  $\omega = 0.8\omega_0$ , at which the PBoCs estimated in (37) and (38) are  $C(1,2) = 4.095 \times 10^{-4}$ , and  $C(3,0) = 302.2338$ , respectively. The results in Figs. 7 and 8 show that when the nonlinear parameter is selected under the estimated bound, the synthesized output can well approximate to the original output, while the synthesized output becomes divergent when the corresponding parameters take larger values.

Eq. (24) can be used to estimate the convergence margin indicator  $\Gamma$ . Firstly, according to (25), the following equations hold:

$$\begin{aligned} a_{1,3} &= C(3,0), & a_{1,1} &= C(1,2)U^2 - \underline{L}(\omega), & a_{1,0} &= \overline{H}_1(j\omega)U\underline{L}(\omega), \\ a_{2,2} &= 3C(3,0), & a_{2,0} &= (C(1,2)U^2 - \underline{L}(\omega))\Gamma, \end{aligned}$$

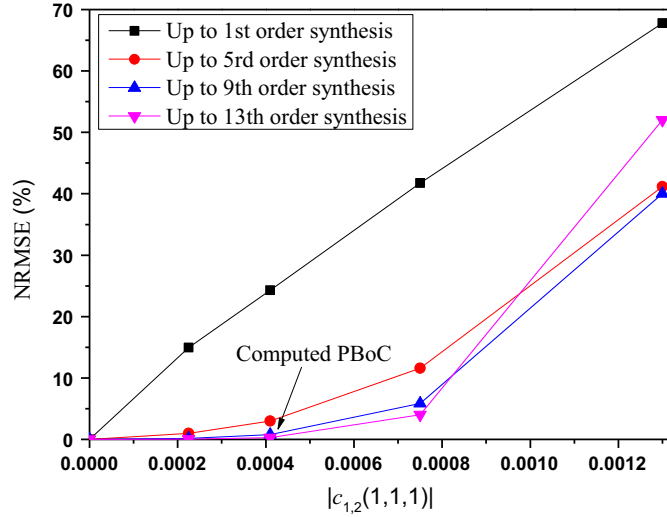


Fig. 7. Comparison of the synthesized output and the original output at  $\omega = 0.8\omega_0$  with  $c_{3,0}(1, 1, 1) = -153.8223$ .

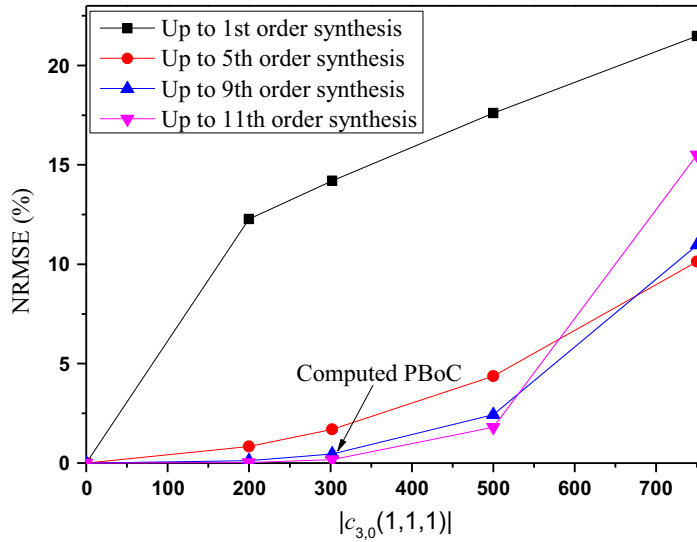


Fig. 8. Comparison of the synthesized output and the original output at  $\omega = 0.8\omega_0$  with  $c_{1,2}(1, 1, 1) = -1.5382 \times 10^{-4}$ .

$$a_{1,2} = a_{2,1} = 0.$$

Then  $\Gamma$  satisfies the following equation according to (24):

$$\begin{vmatrix} C(3,0) & 0 & C(1,2)U^2 - \underline{L}(\omega) & \bar{H}_1(j\omega)U\underline{L}(\omega) & 0 \\ 0 & C(3,0) & 0 & C(1,2)U^2 - \underline{L}(\omega) & \bar{H}_1(j\omega)U\underline{L}(\omega) \\ 3C(3,0) & 0 & \Gamma(C(1,2)U^2 - \underline{L}(\omega)) & 0 & 0 \\ 0 & 3C(3,0) & 0 & \Gamma(C(1,2)U^2 - \underline{L}(\omega)) & 0 \\ 0 & 0 & 3C(3,0) & 0 & \Gamma(C(1,2)U^2 - \underline{L}(\omega)) \end{vmatrix} = 0. \quad (39)$$

From (39), the following equation holds:

$$(\underline{L}(\omega))^3 \Gamma^3 - 3(\underline{L}(\omega))^2 C(1,2)U^2 \Gamma^2 + 3\underline{L}(\omega)(C(1,2)U^2)^2 \Gamma - (C(1,2)U^2)^3 + \frac{27C(3,0)(\underline{L}(\omega)\bar{H}_1(j\omega)U)^2}{4} = 0 \quad (40)$$

Then the convergence margin indicator  $\Gamma$  can be solved. When  $\Gamma \geq 1$ , the Volterra series expansion is divergent with  $PCM < 0$ , which is denoted by  $PCM=0$  in the figures. The convergence margin,  $PCM$ , can then be obtained according to (23). The result when  $U = 0.5$ ,  $c_{3,0}(1, 1, 1) = -153.8223$  and  $c_{1,2}(1, 1, 1) = -1.5382 \times 10^{-4}$  is presented in Fig. 9.

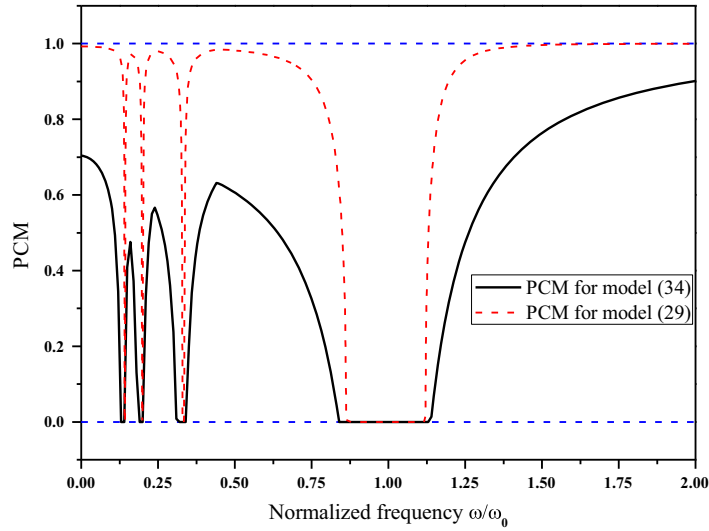


Fig. 9. The parametric convergence margin (PCM) for model (34).

From Fig. 9, the convergence margin PCM with given coefficients and input amplitude is equal to 0 around the resonant and also some harmonic resonance frequencies, and the influence of the nonlinear cross-term with index  $p=1$  can be seen. The nonlinear cross-term gives rise to a stronger nonlinear behavior, which can be observed from the smaller PCM. The width of the frequency band where the PCM=0 around the resonant frequency increases (compared with the case in Section 6.1). This means that the nonlinear dynamic response of the NARX model becomes more complicated after introducing new nonlinear term. Numerical simulations can show that at the frequency with PCM = 0 the system exhibits complicated nonlinear behavior.

### 6.3. The NARX model with pure input nonlinearity and cross nonlinearity

The system model is given by the following:

$$y(k) = c_{1,0}(1)y(k-1) + c_{1,0}(2)y(k-2) + c_{1,2}(1, 1, 1)y(k-1)u^2(k-1) + c_{0,3}(1, 1, 1)u^3(k-1) + c_{0,1}(1)u(k-1) \quad (41)$$

Eqs. (22) and (19) can be used for the computation of the PBoC and PCM, respectively. It is interesting to see that the pure input nonlinear term with coefficient  $c_{0,3}(1, 1, 1)$  does not affect the PBoC of  $c_{1,2}(1, 1, 1)$ , the PBoC of the input magnitude, and the PCM.

From (22), the convergent bound can be obtained,

$$\frac{C(1, 2)U^2}{\underline{L}(\omega)} = 1. \quad (42)$$

The PBoC for  $c_{1,2}(1, 1, 1)$  when  $U = 0.5$  is presented in Fig. 10. The PBoC of  $c_{1,2}(1, 1, 1)$  is very close to 0 at or around harmonic resonance frequencies. In order to validate that the convergent bound (PBoC of  $C(1, 2) = |c_{1,2}(1, 1, 1)|$ ) is independent of the pure input nonlinear parameter, the case that  $c_{0,3}(1, 1, 1) = 0$  and the case that  $c_{0,3}(1, 1, 1) = -2.5 \times 10^{-5}$  are compared. In both cases, the simulations take the same input magnitude and consider the same frequency point, i.e.,  $U = 0.5$ , and  $\omega = 0.8\omega_0$ . The PBoC of  $C(1, 2)$  is computed as 0.00142. The results are presented in Figs. 11 and 12, which show that when  $|c_{1,2}(1, 1, 1)|$  is out of the estimated bound, the synthesized output is divergent, and the convergent bound is independent of  $c_{0,3}(1, 1, 1)$ .

The indicator  $\Gamma$  can be obtained from (19). When  $c_{1,2}(1, 1, 1) = -1.5382 \times 10^{-4}$  and  $U = 0.5$ , the result of the PCM is shown in Fig. 13. The PCM at/around resonant frequency decreases to 0, indicating complicated nonlinear dynamics there.

### 6.4. The NARX model with pure input nonlinearity and pure output nonlinearity

The system model is given by the following:

$$y(k) = c_{1,0}(1)y(k-1) + c_{1,0}(2)y(k-2) + c_{3,0}(1, 1, 1)y^3(k-1) + c_{0,3}(1, 1, 1)u^3(k-1) + c_{0,1}(1)u(k-1) \quad (43)$$

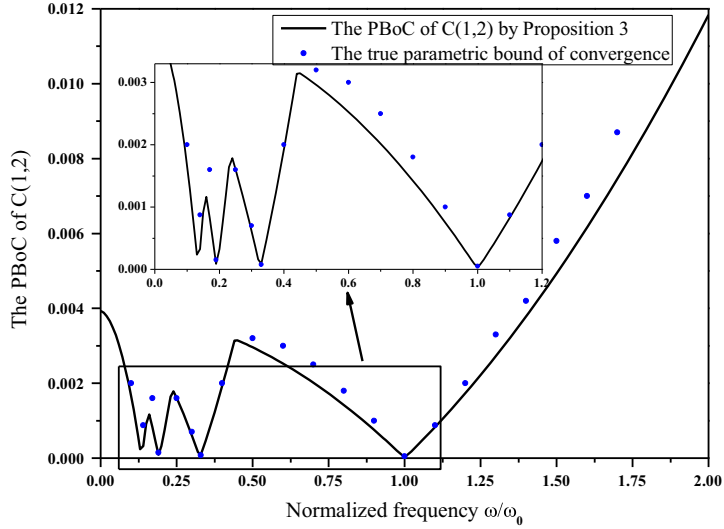


Fig. 10. The PBoC of  $C(1,2) = |c_{1,2}(1, 1, 1)|$ .

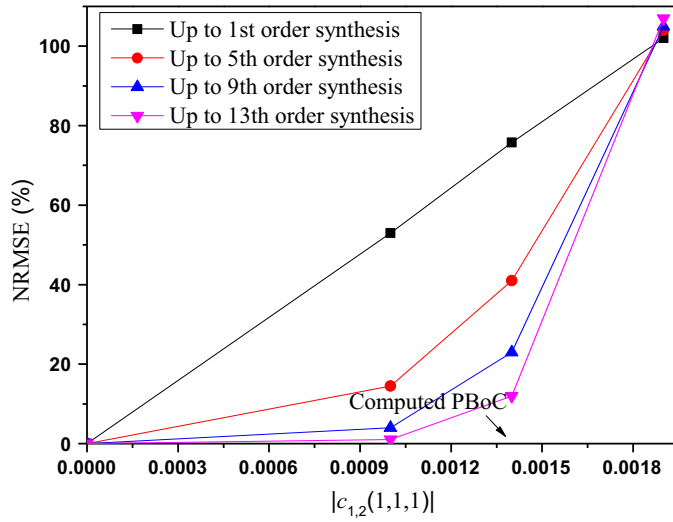


Fig. 11. Comparison of the synthesized output and the original output at  $\omega = 0.8\omega_0$  with  $c_{0,3}(1, 1, 1) = 0$ .

This example is given as a comparison to Sections 6.1 and 6.3 to show further how the pure input nonlinearity affects the PBoC and the PCM. In this case, (20) works for the calculation of the PBoC. From (21),

$$\begin{aligned} a_{1,3} &= 2C(3, 0), & a_{1,0} &= -C(0, 3)U^3 - \bar{H}_1(j\omega)U\underline{L}(\omega), \\ a_{2,2} &= 3C(3, 0), & a_{2,0} &= -\underline{L}(\omega), \\ a_{1,2} &= a_{1,1} = a_{2,1} = 0. \end{aligned}$$

Then the convergent bounds satisfy the following equation:

$$\begin{vmatrix} 2C(3,0) & 0 & 0 & -C(0,3)U^3 - \bar{H}_1(j\omega)U\underline{L}(\omega) & 0 \\ 0 & 2C(3,0) & 0 & 0 & -C(0,3)U^3 - \bar{H}_1(j\omega)U\underline{L}(\omega) \\ 3C(3,0) & 0 & -\underline{L}(\omega) & 0 & 0 \\ 0 & 3C(3,0) & 0 & -\underline{L}(\omega) & 0 \\ 0 & 0 & 3C(3,0) & 0 & -\underline{L}(\omega) \end{vmatrix} = 0 \quad (44)$$

From (44), the following equation can be obtained:

$$(\underline{L}(\omega))^3 - \frac{27}{4}C(3,0)(\bar{H}_1(j\omega)U\underline{L}(\omega) + C(0,3)U^3)^2 = 0 \quad (45)$$

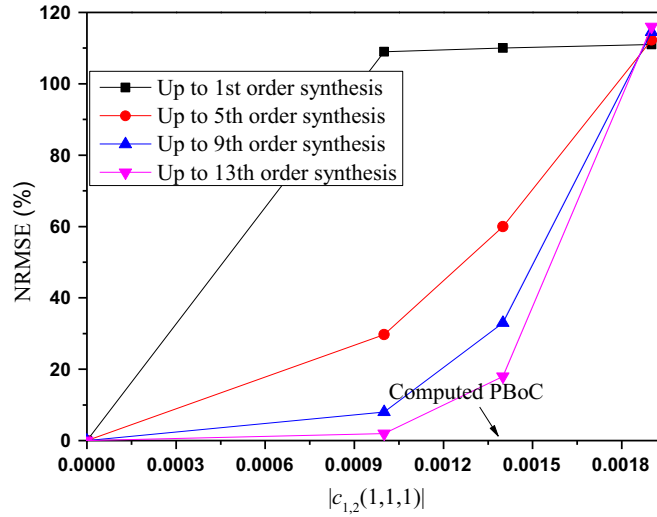


Fig. 12. Comparison of the synthesized output and the original output at  $\omega = 0.8\omega_0$  with  $c_{0,3}(1, 1, 1) = -2.5 \times 10^{-5}$ .

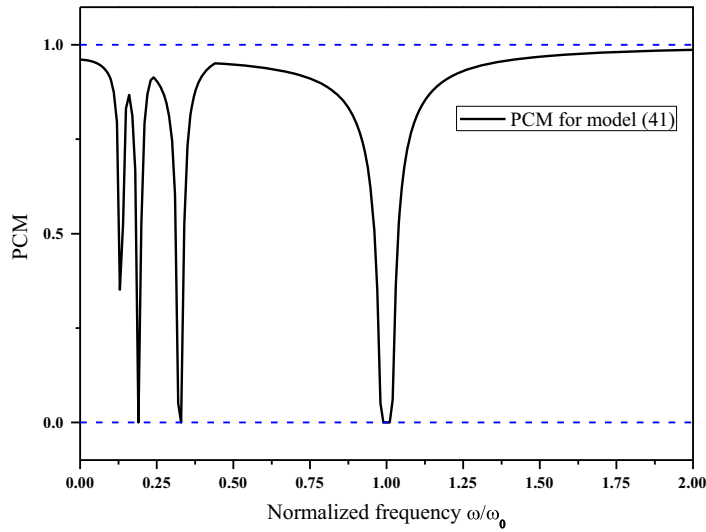


Fig. 13. The PCM for model (41).

It shows the relationship among different parameter bounds (i.e.,  $U$ ,  $C(3, 0)$  and  $C(0, 3)$ ). With the other parameters given, the bound of the remaining one can be obtained,

$$C(3, 0) = \frac{4}{27} \frac{(\underline{L}(\omega))^3}{(\overline{H}_1(j\omega)U\underline{L}(\omega) + C(0, 3)U^3)^2} \quad (46)$$

$$C(0, 3) = \frac{\sqrt{(4(\underline{L}(\omega))^3/27C(3, 0)) - \overline{H}_1(j\omega)U\underline{L}(\omega)}}{U^3}. \quad (47)$$

From (46), it is clear that the coefficient of the pure input nonlinearity (i.e.,  $c_{0,3}(1, 1, 1)$ ) does affect the estimation of the bound of  $C(3, 0)$ , and from (47) it is shown that the bound of  $C(0, 3)$  also affects the estimation of the bound of  $C(3, 0)$ . This is different from the case in Section 6.3 where the pure input nonlinearity has no effect on the PBoC.

The estimated PBoCs for  $C(3, 0)$  and  $C(0, 3)$  are shown in Figs. 14 and 15, respectively, with  $c_{0,3}(1, 1, 1) = -2.3073 \times 10^{-7}$  in Fig. 14,  $c_{3,0}(1, 1, 1) = -153.8223$  in Fig. 15. The proposed method can give close computations for the PBoC around harmonic resonance frequencies both in Figs. 14 and 15. In Fig. 14 the computed PBoC of  $C(3, 0)$  is very close to 0 around all harmonic frequencies, while in Fig. 15 the PBoC of  $C(0, 3)$  becomes 0 in the frequency bands around some of these frequencies.

The validation of these estimated bounds is given in Figs. 16 and 17 with  $\omega = 0.8\omega_0$  and  $U = 0.5$  in the simulations. Given the model parameters  $c_{0,3}(1, 1, 1) = -2.3073 \times 10^{-7}$  for (46) and  $c_{3,0}(1, 1, 1) = -153.8223$  for (47). The PBoCs are computed

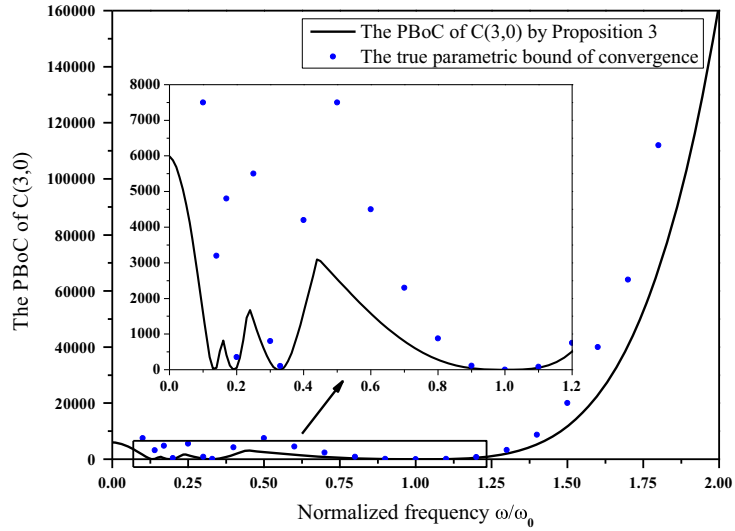


Fig. 14. The PBoC of  $C(3, 0) = |c_{3,0}(1, 1, 1)|$ .

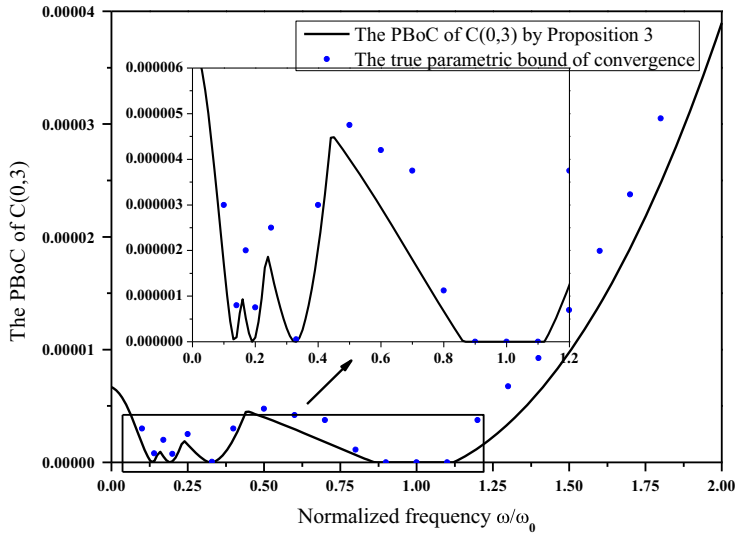


Fig. 15. The PBoC of  $C(0, 3) = |c_{0,3}(1, 1, 1)|$ .

as  $C(3,0)=281.2949$  and  $C(0,3)=6.6431 \times 10^{-7}$ . Figs. 16 and 17 show that the estimated bound is very effective and the synthesized output becomes slowly divergent when the nonlinear coefficients are out of the estimated bound.

For the calculation of the PCM, firstly, the following equations hold from (25):

$$a_{1,3} = C(3, 0), \quad a_{1,1} = -\underline{L}(\omega), \quad a_{1,0} = C(0, 3)U^3 + \overline{H}_1(j\omega)U\underline{L}(\omega)$$

$$a_{2,2} = 3C(3, 0), \quad a_{2,0} = -\underline{\Gamma}L(\omega),$$

$$a_{1,2} = a_{2,1} = 0.$$

Then from (24), it can be obtained that

$$\begin{vmatrix} C(3, 0) & 0 & -\underline{L}(\omega) & C(0, 3)U^3 + \overline{H}_1(j\omega)U\underline{L}(\omega) & 0 \\ 0 & C(3, 0) & 0 & -\underline{L}(\omega) & C(0, 3)U^3 + \overline{H}_1(j\omega)U\underline{L}(\omega) \\ 3C(3, 0) & 0 & -\underline{\Gamma}L(\omega) & 0 & 0 \\ 0 & 3C(3, 0) & 0 & -\underline{\Gamma}L(\omega) & 0 \\ 0 & 0 & 3C(3, 0) & 0 & -\underline{\Gamma}L(\omega) \end{vmatrix} = 0$$



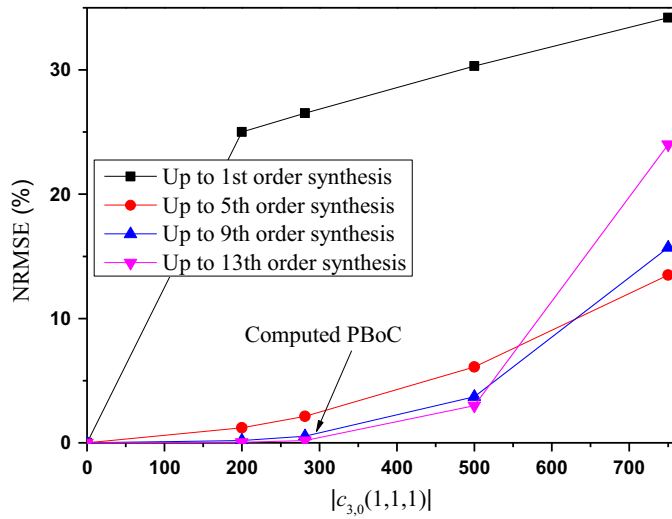


Fig. 16. Comparison of the synthesized output and the original output at  $\omega = 0.8\omega_0$  with  $c_{0,3}(1, 1, 1) = -2.3073 \times 10^{-7}$ .

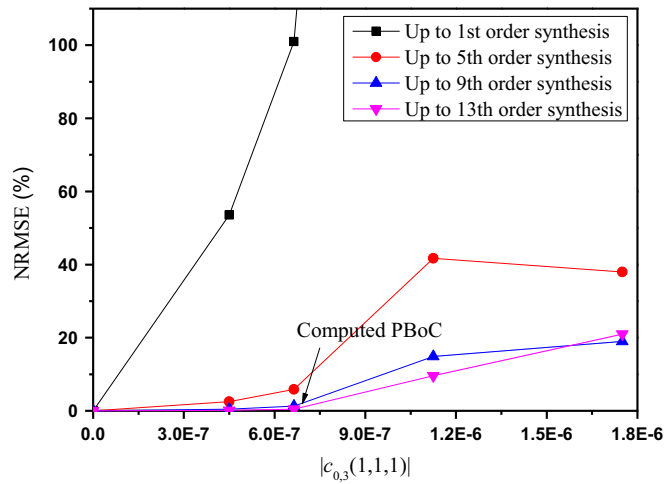


Fig. 17. Comparison of the synthesized output and the original output at  $\omega = 0.8\omega_0$  with  $c_{3,0}(1, 1, 1) = -153.8223$ .

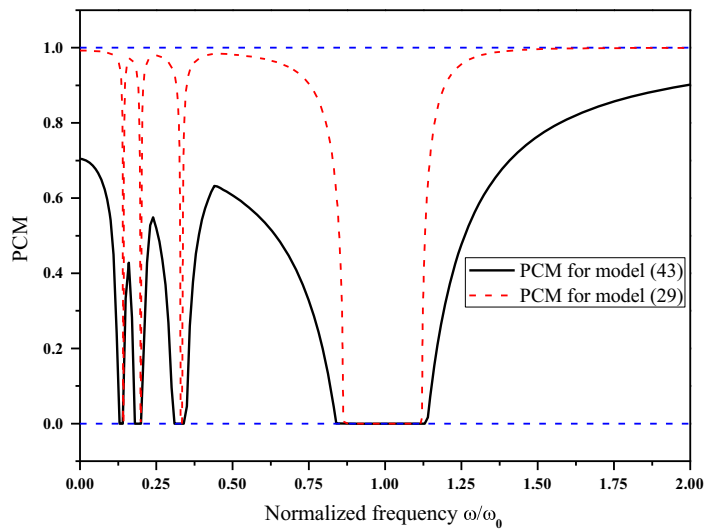


Fig. 18. The PCM for system (43).

from which the convergence margin indicator  $\Gamma$  can be obtained,

$$\Gamma = \frac{1}{\underline{L}(\omega)} \times \left( \frac{27C(3, 0)(\underline{L}(\omega)\bar{H}_1(j\omega)U + C(0, 3)U^3)^2}{4} \right)^{1/3} \tag{48}$$

When  $U = 0.5$ ,  $c_{3,0}(1, 1, 1) = -153.8223$  and  $c_{0,3}(1, 1, 1) = -2.3073 \times 10^{-7}$ , the convergence margin is presented in Fig. 18. From Fig. 18, it can be seen that the introduced pure input nonlinear term causes a smaller PCM, which means that it gives rise to stronger nonlinear behavior. The PCM around the super harmonic resonance frequencies decreases to 0 and the region where PCM = 0 becomes wider, implying that the nonlinear dynamics becomes more complicated.

**7. Conclusion**

The concepts PBoC and PCM are proposed and investigated for quantitative assessment on whether a given nonlinear system has a convergent Volterra series expansion, and for evaluation of the nonlinear severity in the system. The PBoC is a bound of a characteristic parameter, under which the output response of any given NARX model can be well approximated by a convergent Volterra series expansion; while the PCM can evaluate the extent to which the system has a convergent Volterra series expansion at any frequency. The computation of them can all be done easily with respect to any characteristic parameter of interest (including model parameters, input magnitude, and frequency variable) without iterative calculation. The results presented in this study should provide a fundamental basis and useful guidance for nonlinear analysis and design both in the time and frequency domains using the Volterra series based theory and methods.

**Acknowledgment**

The authors would like to thank the handling editor and anonymous reviewers for their useful comments and constructive suggestions on this paper. The authors would also like to acknowledge the support from the NSFC project (Ref 61374041) of China, GRF project (Ref 517810) of Hong Kong RGC, Department General Research Funds and internal Research Grants of Hong Kong Polytechnic University.

**Appendix A. Proof of Proposition 1**

$$\begin{aligned} & \frac{1}{\underline{L}(\omega)} \sum_{m=2}^{+\infty} \sum_{p=1}^m U^q C(p, q) (\bar{Y}(U)_\omega)^p + \frac{1}{\underline{L}(\omega)} \sum_{q=m=2}^{+\infty} C(0, m) U^m \\ &= \frac{1}{\underline{L}(\omega)} \sum_{m=2}^{+\infty} \sum_{p=1}^m C(p, q) \left( \sum_{i=1}^{+\infty} \bar{H}_i(j\omega_1, \dots, j\omega_i) U^i \right)^p U^q + \frac{1}{\underline{L}(\omega)} \sum_{q=m=2}^{+\infty} C(0, m) U^m \\ &= \sum_{n=2}^{+\infty} \left( \frac{1}{\underline{L}(\omega)} \left( C(0, n) + \sum_{m=2}^n \sum_{p=1}^m C(p, q) \sum_{r_1=1, \sum r_i=n-q}^{n-m+1} \prod_{i=1}^p \bar{H}_{r_i}(j\omega_1, \dots, j\omega_{r_i}) \right) \right) U^n \\ &= \sum_{n=2}^{+\infty} \bar{H}_n(j\omega_1, \dots, j\omega_n) U^n \end{aligned}$$

then, the following equation holds:

$$\frac{1}{\underline{L}(\omega)} \sum_{m=2}^{+\infty} \sum_{p=1}^m U^q C(p, q) (\bar{Y}(U)_\omega)^p + \frac{1}{\underline{L}(\omega)} \sum_{q=m=2}^{+\infty} C(0, m) U^m = \bar{Y}(U)_\omega - \bar{H}_1(j\omega)U, \quad p+q \geq 2 \tag{A.1}$$

Denote  $x(\omega, U) = \bar{Y}(U)_\omega = \sum_{n=1}^{+\infty} \bar{H}_n(j\omega_1, \dots, j\omega_n) U^n$ , and rearrange (A.1), (17) can be obtained. The result in (18) is straightforward according to (17).

This completes the proof.

**Appendix B. Proof of Proposition 2**

When the input amplitude  $U$  increases with the model parameters fixed, the upper bound of the nonlinear output spectrum  $x = \sum_{n=1}^{+\infty} \bar{H}_n(j\omega_1, \dots, j\omega_n) U^n$  also increases. When any nonlinear model parameter increases with the other model parameters and the input amplitude  $U$  fixed, according to (14), the bound of the  $n$ th order GFRF  $\bar{H}_n(j\omega_1, \dots, j\omega_n)$  also increases. Therefore, the upper bound of the nonlinear output spectrum  $x$  increases accordingly. Both these cases make the function  $\Gamma$  increase.

It is clear that  $\Gamma = 0$  when the input amplitude  $U = 0$  or all the nonlinear model parameters are zero ( $C(p, q) = 0$ ). When the Volterra series expansion is divergent, the upper bound of the nonlinear output spectrum  $x \rightarrow \infty$ , thus

$$\Gamma = \frac{1}{\underline{L}(\omega)} \sum_{p=1}^{M_p} \sum_{q=0}^{\infty} p C(p, q) U^q x^{p-1} \rightarrow \infty.$$

For the case that only the nonlinear terms with index  $p=1$  or together with the pure input nonlinear terms are included in the NARX model, it is obvious that there exist some  $(U, C(1, q))$  such that  $\Gamma = (1/\underline{L}(\omega)) \sum_{q=1}^{\infty} C(1, q) U^q > 1$  holds. Because  $\Gamma$  is a continuous and monotonically increasing function with respect to the input amplitude  $U$  or any nonlinear model parameter, then  $\Gamma = 1$  exists for some  $U$  and  $C(p, q)$ .

According to (11)–(13), it is clear that  $\underline{L}(\omega)$ ,  $\bar{H}_1(j\omega)$ , and  $C(p, q)$  are no functions of the input amplitude  $U$ . When the model parameters are given, the upper bound of the nonlinear output spectrum is only a function of the input magnitude  $U$ . Calculate the derivative with respect to  $U$  in (17), the following equation holds:

$$\sum_{p=1}^{M_p} \sum_{q=0}^{\infty} C(p, q) q U^{q-1} x^p + \sum_{p=1}^{M_p} \sum_{q=0}^{\infty} C(p, q) U^q p x^{p-1} \frac{dx}{dU} - \underline{L}(\omega) \frac{dx}{dU} + \underline{L}(\omega) \bar{H}_1(j\omega) + \sum_{m=2}^{\infty} C(0, m) m U^{m-1} = 0, \quad p+q \geq 2.$$

From this equation,  $dx/dU$  can be obtained. And then the derivative of the inverse function  $U(x)$  is given by the following:

$$\frac{dU}{dx} = \frac{1}{dx/dU} = \frac{\underline{L}(\omega) - \sum_{p=1}^{M_p} \sum_{q=0}^{\infty} C(p, q) U^q p x^{p-1}}{\sum_{p=1}^{M_p} \sum_{q=0}^{\infty} C(p, q) q U^{q-1} x^p + \underline{L}(\omega) \bar{H}_1(j\omega)}.$$

When  $\Gamma = 1$ , according to (19),  $\sum_{p=1}^{M_p} \sum_{q=0}^{\infty} C(p, q) U^q p x^{p-1} = \underline{L}(\omega)$  holds. Because  $\underline{L}(\omega)$ ,  $\bar{H}_1(j\omega)$ ,  $C(p, q)$  and  $U$  are nonnegative, thus the denominator is always larger than 0, and then  $dU/dx = 0$  holds.

According to the Analytic Inversion Lemma in [33]: An analytic function locally admits an analytic inverse near any point where its first derivative is non-zero. However, a function cannot be analytically inverted in a neighborhood of a point where its first derivative vanishes. Because the output bound  $x = \sum_{n=1}^{+\infty} \bar{H}_n(j\omega_1, \dots, j\omega_n) U^n$  is a power series of input amplitude  $U$ , and it is known that the power series is analytic in the convergence region, which means that there does not exist singularity in the convergence region.

From the discussion above, when  $0 \leq \Gamma < 1$ ,  $dU/dx \neq 0$  holds, which means that no singularity exists in this region, thus  $x$  (described by an infinite power series  $x = \sum_{n=1}^{+\infty} \bar{H}_n(j\omega_1, \dots, j\omega_n) U^n$ ) is convergent in this region. When  $\Gamma = 1$ , the output bound  $x$  is divergent. Because  $\Gamma$  increases as the input amplitude  $U$  increases or the nonlinear model parameters function  $C(p, q)$  increases, so when  $\Gamma > 1$ , there exists a smaller input amplitude  $U$  or smaller function  $C(p, q)$  which can bring  $\Gamma$  back to  $\Gamma = 1$ , clearly indicating that the output bound  $x$  is divergent for  $\Gamma > 1$ .

This completes the proof.

**Remark 9.** Technically, the proof above is based on the Analytic Combinatorics in [33] and a similar idea was already demonstrated in [23]. However, the results of this study cannot be seen as a straightforward extension of [23] by noticing the following facts. The results in Lemma 2 are presented in power series, which cannot be obtained without the bound result of the output spectrum, and also the derivation in the proof of Lemma 2 is totally different from that in [23]. The computation of the magnitude bound of the output spectrum in Proposition 1 is presented analytically in algebraic polynomial with explicit coefficients, which is obtained based on Lemma 1. In the proof of Proposition 1, the polynomial constructed is different from that in [23], and the key point of the derivation is mainly based on the result in Lemma 1. The indicator  $\Gamma$  in Proposition 2 is the first time proposed to express whether the nonlinear system is convergent or not in the sense of Volterra series expansion, the key point of the proof of Proposition 2 is based on the Analytic Inversion Lemma in page 260 in [33], while the main convergence result and the proof of the result in [23] mainly follow the Singular Inversion Theorem in p. 262 and p. 383 in [33]. Finally, in [23], the input should be affine and the result is only limited to calculate the input bound. But in this study, the input can be any nonlinearity in polynomial form, and the result is more general, which cannot only compute the input magnitude bound but also the parameter bounds.

### Appendix C. Proof of Proposition 3

The upper bound of the nonlinear output spectrum  $x$  reaches the convergent bound when  $\Gamma = 1$  holds. In the case that the NARX model does not only involve the type of nonlinear term with index  $p=1$  or together with the pure input nonlinear term, the following condition holds:

$$\sum_{p=1}^{M_p} \left( p \sum_{q=0}^{\infty} C(p, q) U^q \right) x^{p-1} = \underline{L}(\omega), \quad p+q \geq 2, \quad (C.1)$$

By substituting (C.1) into (17), it can be obtained that

$$\sum_{p=1}^{M_p} \left( (p-1) \sum_{q=0}^{\infty} C(p, q) U^q \right) x^p = \underline{L}(\omega) \bar{H}_1(j\omega) U + \sum_{m=2}^{\infty} C(0, m) U^m, \quad p+q \geq 2, \quad (C.2)$$

Define the formal function  $f(x) = a_n x^n + \dots + a_1 x + a_0$ , and  $g(x) = b_m x^m + \dots + b_1 x + b_0$ . The Sylvester matrix of  $f(x)$  and  $g(x)$  is defined as follows:

$$\text{Syl}(f, g) = \begin{matrix} m \text{ rows} \\ n \text{ rows} \end{matrix} \left\{ \begin{matrix} \begin{bmatrix} a_n & \dots & a_0 \\ & \dots & \\ & & a_n & a_0 \end{bmatrix} \\ \begin{bmatrix} b_m & \dots & b_0 \\ & \dots & \\ & & b_m & \dots & b_0 \end{bmatrix} \end{matrix} \right\}_{(m+n) \times (m+n)} \tag{C.3}$$

The sufficient and necessary condition for the existence of a solution to the equations

$$\begin{cases} f(x) = 0 \\ g(x) = 0 \end{cases}$$

is that the Sylvester Resultant equals to 0 [34], that is,

$$\text{Res}(f, g) = \det(\text{Syl}(f, g)) = 0 \tag{C.4}$$

where  $\det(\cdot)$  means the determinant of the matrix, and  $\text{Res}(\cdot)$  means the Sylvester Resultant of the functions. Eqs. (C.1) and (C.2) are rewritten as follows:

$$\begin{cases} \sum_{p=1}^{M_p} \left( (p-1) \sum_{q=0}^{\infty} C(p, q) U^q \right) x^p = \underline{L}(\omega) \bar{H}_1(j\omega) U + \sum_{m=2}^{\infty} C(0, m) U^m \\ \sum_{p=1}^{M_p} \left( p \sum_{q=0}^{\infty} C(p, q) U^q \right) x^{p-1} = \underline{L}(\omega) \end{cases}, \quad p+q \geq 2, \tag{C.5}$$

Eq. (17) always holds no matter whether  $x$  is convergent or divergent. If there exists a  $(C(p, q), U, \underline{L}(\omega), x)$  that satisfies (C.1), it also satisfies (17), and thus (C.2) holds for this  $(C(p, q), U, \underline{L}(\omega), x)$ . Therefore, there exists an  $x$  that satisfies (C.5). Then according to the analysis above, (C.4) holds (the Sylvester Resultant is equal to 0 in this case). According to (C.5), the Sylvester matrix in (C.3) and (C.4) can be obtained by defining the elements in (21).

For the case that the NARX model only involves the type of nonlinear terms with  $p=1$  and the pure input nonlinear term, the result in (22) is straightforward.

This completes the proof.

Appendix D. Proof of Proposition 4

Rearrange (19), the following equation holds:

$$\sum_{p=1}^{M_p} \left( p \sum_{q=0}^{\infty} C(p, q) U^q \right) x^{p-1} - \Gamma \underline{L}(\omega) = 0, \quad p+q \geq 2, \tag{D.1}$$

If there is a  $(C(p, q), U, \underline{L}(\omega), x, \Gamma)$  that satisfies (D.1), the corresponding part, i.e.  $(C(p, q), U, \underline{L}(\omega), x)$  also satisfies (17). Thus there exists a solution for  $x$  in the following equations:

$$\begin{cases} \sum_{p=1}^{M_p} \left( \sum_{q=0}^{\infty} C(p, q) U^q \right) x^p - \underline{L}(\omega) x + \underline{L}(\omega) \bar{H}_1(j\omega) U + \sum_{m=2}^{\infty} C(0, m) U^m = 0 \\ \sum_{p=1}^{M_p} \left( p \sum_{q=0}^{\infty} C(p, q) U^q \right) x^{p-1} - \Gamma \underline{L}(\omega) = 0 \end{cases}, \quad p+q \geq 2 \tag{D.2}$$

which means that the Sylvester Resultant of Eq. (D.2) is equal to 0, and then similarly to Appendix C, (24) and (25) hold.

For the case of the NARX model with only the type of nonlinear terms with index  $p=1$  or together with pure input nonlinearity, the result is straightforward.

This completes the proof. □

References

[1] S. Chen, S.A. Billings, Representations of non-linear systems: the NARMAX model, *Int. J. Control* 49 (1989) 1013–1032.  
 [2] I.J. Leontaritis, S.A. Billings, Input-output parametric models for non-linear systems Part I: deterministic non-linear systems, *Int. J. Control* 41 (1985) 303–328.  
 [3] I.J. Leontaritis, S.A. Billings, Input-output parametric models for non-linear systems Part II: stochastic non-linear systems, *Int. J. Control* 41 (1985) 329–344.  
 [4] D. Jiang, C. Pierre, S.W. Shaw, Nonlinear normal modes for vibratory systems under harmonic excitation, *J. Sound Vib.* 288 (2005) 791–812.

- [5] G. Kerschen, M. Peeters, J.C. Golinval, A.F. Vakakis, Nonlinear normal modes, Part I: a useful framework for the structural dynamicist, *Mech. Syst. Signal Process.* 23 (2009) 170–194.
- [6] M. Peeters, R. Vigué, G. Sérandour, G. Kerschen, J.C. Golinval, Nonlinear normal modes, Part II: toward a practical computation using numerical continuation techniques, *Mech. Syst. Signal Process.* 23 (2009) 195–216.
- [7] X.J. Jing, Z.Q. Lang, S.A. Billings, G.R. Tomlinson, The parametric characteristic of frequency response functions for nonlinear systems, *Int. J. Control* 79 (2006) 1552–1564.
- [8] D.A. George, *Continuous Nonlinear Systems*, DTIC Document, 1959.
- [9] I. Sandberg, The mathematical foundations of associated expansions for mildly nonlinear systems, *IEEE Trans. Circ. Syst.* 30 (1983) 441–455.
- [10] I. Sandberg, Expansions for nonlinear systems, *Bell Syst. Tech. J.* 61 (1982) 159–199.
- [11] S. Boyd, L. Chua, Fading memory and the problem of approximating nonlinear operators with Volterra series, *IEEE Trans. Circ. Syst.* 32 (1985) 1150–1161.
- [12] W.J. Rugh, *Nonlinear System Theory*, Johns Hopkins University Press, Baltimore, MD, 1981.
- [13] P. Marzocca, J.M. Nichols, A. Milanese, An analytical formulation of bispectral densities for multiple degree-of-freedom systems, *J. Eng. Math.* 67 (2010) 351–367.
- [14] J.M. Nichols, P. Marzocca, A. Milanese, The trispectrum for Gaussian driven, multiple degree-of-freedom, non-linear structures, *Int. J. Non Linear Mech.* 44 (2009) 404–416.
- [15] J.M. Nichols, P. Marzocca, A. Milanese, On the use of the auto-bispectral density for detecting quadratic nonlinearity in structural systems, *J. Sound Vib.* 312 (2008) 726–735.
- [16] P. Marzocca, J.M. Nichols, A. Milanese, M. Seaver, S.T. Trickey, Second-order spectra for quadratic nonlinear systems by Volterra functional series: analytical description and numerical simulation, *Mech. Syst. Signal Process.* 22 (2008) 1882–1895.
- [17] I. Sandberg, On Volterra expansions for time-varying nonlinear systems, *IEEE Trans. Circ. Syst.* 30 (1983) 61–67.
- [18] S. Boyd, L. Chua, C. Desoer, Analytical foundations of Volterra series, *IMA J. Math. Control Inf.* 1 (1984) 243–282.
- [19] G.R. Tomlinson, G. Manson, G.M. Lee, A simple criterion for establishing an upper limit to the harmonic excitation level of the Duffing oscillator using the Volterra series, *J. Sound Vib.* 190 (1996) 751–762.
- [20] Z.K. Peng, Z.Q. Lang, On the convergence of the Volterra-series representation of the Duffing's oscillators subjected to harmonic excitations, *J. Sound Vib.* 305 (2007) 322–332.
- [21] L.M. Li, S.A. Billings, Analysis of nonlinear oscillators using Volterra series in the frequency domain, *J. Sound Vib.* 330 (2011) 337–355.
- [22] F. Bullo, Series expansions for analytic systems linear in control, *Automatica* 38 (2002) 1425–1432.
- [23] T. Helie, B. Laroche, Computation of convergence bounds for Volterra series of linear-analytic single-input systems, *IEEE Trans. Autom. Control* 56 (2011) 2062–2072.
- [24] J.C.P. Jones, S.A. Billings, Recursive algorithm for computing the frequency response of a class of non-linear difference equation models, *Int. J. Control* 50 (1989) 1925–1940.
- [25] Z.-Q. Lang, S.A. Billings, Output frequency characteristics of nonlinear systems, *Int. J. Control* 64 (1996) 1049–1067.
- [26] X.J. Jing, Z.Q. Lang, S.A. Billings, New bound characteristics of NARX model in the frequency domain, *Int. J. Control* 80 (2006) 140–149.
- [27] X.J. Jing, Z.Q. Lang, S.A. Billings, Output frequency properties of nonlinear systems, *Int. J. Non Linear Mech.* 45 (2010) 681–690.
- [28] X. Jing, Z. Lang, On the generalized frequency response functions of Volterra systems, *J. Dyn. Syst. Meas. Control* 131 (2009) 061002.
- [29] Z. Xiao, X. Jing, L. Cheng, Parameterized convergence bounds for Volterra series expansion of NARX models, *IEEE Trans. Signal Process.* 61 (2013) 5026–5038.
- [30] S. Billings, O. Boaghe, The response spectrum map, a frequency domain equivalent to the bifurcation diagram, *Int. J. Bifurc. Chaos* 11 (2001) 1961–1975.
- [31] O.M. Boaghe, S.A. Billings, Subharmonic oscillation modeling and MISO Volterra series, *IEEE Trans. Circ. Syst. I: Fundam. Theory Appl.* 50 (2003) 877–884.
- [32] X. Jing, Z. Lang, S. Billings, Parametric characteristic analysis for generalized frequency response functions of nonlinear systems, *Circ. Syst. Signal Process.* 28 (2009) 699–733.
- [33] P. Flajolet, R. Sedgewick, *Analytic Combinatorics*, Cambridge Univ Press, 2009.
- [34] B. Roth, Computations in kinematics, *Comput. Kinemat.* (1993) 3–14.